AGU PUBLICATIONS

Global Biogeochemical Cycles

Supporting Information for

Towards a quantitative and empirical dissolved organic carbon budget for the Gulf of Maine, a semi-enclosed shelf sea

William Balch[1], Thomas Huntington[2], George Aiken[3], David Drapeau[1], Bruce Bowler[1], Laura Lubelczyk[1], Kenna Butler[3]

[1]Bigelow Laboratory for Ocean Sciences, POB 380, 60 Bigelow Dr., East Boothbay, ME 04544

[2]U. S. Geological Survey, 196 Whitten Rd., Augusta, ME 04330

[3]U.S. Geological Survey, 3215 Marine Street, Boulder, Colorado 80303-1066

Contents of this file

Text S1 Supplemental Methods

Table S1

Figures S1 to S8

Introduction

We provide supplemental methods descriptions for the work performed in the aforementioned manuscript (Text S1). This includes methods for: GNATS continuous underway measurements, GNATS discrete measurements and chemical analyses . We also provide eight supplementary figures showing: Fig. S1- DOC concentration versus CDOM absorbance measured across the GOM; Fig. S2- Hövmoller plots (longitude of east-west GNATS transect plotted against year) for various properties; Fig. S3- Mean variables measured over Slocum glider missions (10 complete missions; 20 crossings of the GNATS transect); Fig. S4- Time course of Gulf-wide absorption measurements of CDOM and CDOM plus detrital matter plotted against year; Fig. S5- Time course of Gulf-wide scattering measurements of CDOM and CDOM plus detrital matter plotted against year., Fig S6- Satellite-derived estimates of Gulf-wide DOC concentration plotted against LoadEst estimates of DOC discharge rate from five largest rivers that we used for these analyses (Penobscot, Dennys, St. Croix, Narragauagus and St. John Rivers), Fig S7- Time series of DOC discharge from the five largest rivers emptying into the Gulf of Maine and mean satellite-derived, Gulf-wide average DOC concentration and Fig. S8- Predictions of future annual DOC export from the Penobscot River based on the LOADEST model assuming the Hadley Center Model- A1F1 Emission Scenario.

Text S1. Supplemental Methods

Continuous underway measurements

The instruments used in GNATS for continuous underway measurements of surface water (sampled from 2-3m depth) are: thermosalinograph, WETLabs ac-9 (spectral absorption/attenuation meter), chlorophyll fluorometer, Satlantic SAS (above-water radiometers), Wyatt volume scattering meter, HOBI Labs HydroScat-2 (volume scattering meter), and FlowCam (Fluid Imaging Technologies; Yarmouth, ME) a flow-through microscope/flow cytometer/image analyzer that provides real-time particle size distribution data and phytoplankton species information for particles of 4-200μm). All optical measurements were in strict accordance with NASA protocols [*Mueller et al.*, 2003]. WETLabs ac-9 absorption and attenuation measurements were made with raw seawater, or seawater diverted serially through a 1μm filter followed by a 0.2μm filter (operationally-defined as the "dissolved" fraction). Above-water radiance measurements were made with the 7-channel Satlantic SAS radiometer system. The sea-viewing and sky-viewing radiance sensors were constantly maintained with a viewing angle of 90°-120° from the solar azimuth to minimize sun glint and they were aimed at 40° from nadir and zenith, respectively (as per instrument protocols [*Mueller et al.*, 2003]). The downwelling irradiance sensor was maintained in an elevated portion on all vessels, with minimal ship superstructure above it to prevent shadowing. Water-leaving radiance was calculated according to Mueller et al [2003].

Discrete measurements— Every ~35km across the GoM, nine discrete surface samples were taken from the underway sample stream. The placement of these stations for each trip was planned to be equidistant across the Gulf. If sky conditions were clear, then the exact location of specific stations was moved to match the exact time of overpass of the various NASA ocean color sensors (SeaWiFS, MODIS Terra, MODIS Aqua; NPP VIIRS). This optimized the validation of the various satellite measurements but this meant that 2-3 of the 9 stations each trip were not necessarily at exactly the same location along the GNATS transect (Fig. 1). For each water sample, aliquots were subsampled for PIC [*Poulton et al.*, 2006], POC and chlorophyll *a* [*JGOFS*, 1996], microscope counts with FlowCam [*Poulton and Martin*, 2010], polarized light microscopy [*Balch and Utgoff*, 2009] and DOC (see below). Since 2001, hourly samples were taken for measuring maximum primary production (P_{max}) and calcification (C_{max}), incubated at the laboratory post-cruise in environmental incubators. Twelve-hour incubations were used (from local apparent midnight to local apparent noon). Light levels, photoperiod and average temperature were matched to surface values in the Gulf of Maine for the specific sampling day. The microdiffusion technique was used to measure carbon fixation via photosynthesis and calcification and the 12h rates were corrected to daily rates using previously measured comparisons between 12h and 24h incubations [*Balch et al.*, 2000; *Balch et al.*, 2008; *Paasche and Brubak*, 1994]. The photoadaptive variables, P_{max} and C_{max}, are arguably the most important for determining integrated algal carbon fixation from space. At each station, vertical profiles were made for temperature (with expendable bathythermographs; XBTs) or during years 2001-4, temperature, salinity and chlorophyll fluorescence using a Brooke Ocean Moving Vessel Profiler (Halifax, NS).

DOC analyses— DOC concentrations were determined using an O.I. Analytical Model 700 TOC analyzer via the platinum catalyzed persulfate wet oxidation method [*Aiken et al*., 1992]. Several approaches were used for analyzing and reporting the optical properties of chromophoric

DOM (CDOM). Decadal UV-Visible absorbance (*A*) was measured on bulk DOC samples at room temperature using a quartz cell with a path length of 1 cm on an Agilent Model 8453 photo-diode array spectrophotometer. Decadal absorption (m^{-1}) was recorded at wavelengths of 254, 350, and 412 nm. Note, while the UV bands provide the highest quality optical data for DOC, the 412nm band overlaps with bands on ocean color sensors (e.g. MODIS and SeaWiFS). Specific UV absorbance ($SUVA_{254}$) was obtained by dividing the decadal absorption coefficient at $\lambda = 254$ nm (a_{254}) by DOC concentration. $SUVA_{254}$, which is typically used as an index of DOC aromaticity [*Weishaar et al*., 2003], is reported in units of m^2 (g DOC)$^{-1}$.

Spectral slope (*S*) was calculated by fitting an exponential equation to the absorption spectra between 275-295 nm using

$$a_g(\lambda) = a_g(\lambda_{ref})\, e^{-S(\lambda - \lambda ref)} \qquad (2)$$

where $a_g(\lambda)$ is the Naperian absorption coefficient of CDOM at a specified wavelength, λ_{ref} , is a reference wavelength, and *S* is the slope fitting parameter [*Spencer et al.*, 2008]. Prior studies have shown the $S_{275\text{-}295}$ to be sensitive to changes in DOM source (e.g. riverine vs. estuarine vs. open ocean and composition) [*Helms et al*., 2008].

References

Balch, W. M., and P. Utgoff (2009), Potential interactions among ocean acidification, coccolithophores and the optical properties of seawater, *Oceanography*, *22*(4), 146-159.

Balch, W. M., D. T. Drapeau, and J. Fritz (2000), Monsoonal forcing of calcification in the Arabian Sea, *Deep-Sea Res. II*, *47*, 1301-1337.

Balch, W. M., D. T. Drapeau, B. C. Bowler, E. S. Booth, L. A. Windecker, and A. Ashe (2008), Space-time variability of carbon standing stocks and fixation rates in the Gulf of Maine, along the GNATS transect between Portland, ME and Yarmouth, NS., *J. Plankton Res.*, *30*(2), 119-139.

Gordon, C., C. Cooper, C. A. Senior, H. Banks, J. M. Gregory, T. C. Johns, J. F. B. Mitchell, and R. A. Wood (2000), The simulation of SST, sea ice extents and ocean heat transports in a version of the Hadley Centre coupled model without flux adjustments, *Climate Dynamics*, *16*(2–3), 147–168.

JGOFS (1996), Protocols for the Joint Global Ocean Flux Study (JGOFS) core measurements, in *Report no. 19 of the Joint Global Ocean Flux Study*, edited by A. Knap, p. 170, Scientific committee on oceanic research, international council of scientific unions. Intergovernmental Oceanographic Commission, Bergen, Norway.

Mueller, J. L., et al. (2003), Ocean optics protocols for satellite ocean color sensor validation, Revision 4, Volume III: Radiometric measurements and data analysis protocols. *Rep.*, 78 pp, Goddard Space Flight Center, Greenbelt, MD.

Nakićenović, N. (2000), Special Report on Emissions Scenarios : a special report of Working Group III of the Intergovernmental Panel on Climate Change*Rep.*, Pacific Northwest National Laboratory (PNNL) Environmental Molecular Sciences Laboratory (EMSL), Richland, WA (US), United States.

Paasche, E., and S. Brubak (1994), Enhanced calcification in the coccolithophorid *Emiliania huxleyi* (Haptophyceae) under phosphorus limitation, *Phycologia*, *33*, 324-330.

Pope, V. D., M. L. Gallani, P. R. Rowntree, and R. A. Stratton (2000), The impact of new physical parameterizations in the Hadley Centre climate model—HadCM3, *Clim. Dyn.*, *16*, 123–146.

Poulton, A. J., R. Sanders, P. M. Holligan, T. Adey, M. Stinchcombe, L. Brown, and K. Chamberlain (2006), Phytoplankton mineralisation in the tropical and subtropical Atlantic Ocean, *Global Biogeochem. Cycles*, *20*(4), GB4002, doi:4010.1029/2006GB002712.

Poulton, N. J., and J. L. Martin (2010), Imaging flow cytometry for quantitative phytoplankton analysis - FlowCAM, in *Microscopic and molecular methods for quantitative phytoplankton analysis*, edited by B. Karlson, C. Cusack and E. Bresnan, pp. 49-54, Intergovernmental Oceanographic Commission of UNESCO, Paris, France.

Spencer, R. G. M., G. R. Aiken, K. P. Wickland, R. G. Striegl, and P. J. Hernes (2008), Seasonal and spatial variability in dissolved organic matter quantity and composition from the Yukon River basin, Alaska, *Global Biogeochem. Cycles*, *22*(4).

Supplemental Table

Table S1- List of river discharge and dissolved organic carbon data used in this work.

River, Location, USGS Station ID No.	Drainage Area (km^{-2})	Period of Record, discharge	Period of Record DOC[1]	Number of DOC Samples	Corresponding Figures[2]
St. John River at Mactaquac Dam, 01AK010	39,900	1919 - Present	(2012-2013)	10	2, 9, 10, S6, S7
St. Croix River at Milltown, 01021050	3,768	1959 to Present	(2007-2013)	20	2, 9, 10, S6, S7
Penobscot River at Eddington, Maine, 01036390	20,109	1904-Present	(2004-2013)	132	2, 9, 10, S6, S7
Kennebec River at North Sidney, Maine 01049265	13,993	1978-1993, 2000 - Present	(2004-2013)	67	2
Androscoggin River near Brunswick, Maine, 01059400	8,894	1929-Present	(2004-2013)	72	2
Saco River near Cornish, 01066000	3,349	1916 - Present	(2007-2013)	31	2
Presumpscot River, near West Falmouth, 01064140	1,494	1975-1995, Gage height only 1998 - Present	(2007-2013)	30	2
Merrimack River, 01100000	12,004	1923 - Present	(1998-2000)	29	2
Dennys River[3], 01021200	241	1955 - Present	(2011-2013)	16	10, S6, S7
Narraguagus River, 01022500	588	1948 - Present	,(2011-2013)	17	2, 9, 10, S6, S7
Sheepscot River, 1038000	376	1938 - Present	(2011-2013)	13	2
Total gauged & sampled area (10 largest rivers)	**104,475**				
Total GoM watershed area	**179,008**				
Total ungauged and unsampled area	**74,533**				

[1]Analyses from 1998-2000 are USGS National Water Quality and Assessment (NAWQA) Program (USGS NWIS http://dx.doi.org/10.5066/F7P55KJN)

[2]Numbers correspond to the analyses and figures that included data from the indicated rivers.

[3]The Dennys River was not included in the analyses involving the ten largest rivers draining to the Gulf of Maine, it was used with the analyses involving the five largest rivers from the Penobscot River to the St. John River.

Supplemental Figures

Figure Legend

Fig. S1- DOC concentration versus CDOM absorbance measured across the GOM, measured at A) 412nm (a_{g412}), B) 350nm(a_{g350}) and C) 254nm (a_{g254}). D) Predicted DOC using a_{g254} and spectral slope ($S_{275-295}$) plotted against measured DOC concentration for samples collected from the GoM. Grey-shaded region shows data range. Least-squares fits to the data are shown in each panel.

Fig. S2- Hövmoller plots (longitude of east-west GNATS transect versus year) for (A) DOC concentration (mg C L^{-1}), (B) (a_{g412}; m^{-1}), (C) (a_{gp412}; m^{-1}), (D) POC (µg L^{-1}), (E) particulate backscattering at 532nm (b_{bp532}; m^{-1}) and (F) dissolved total scattering at 412nm. Color scale bars shown to right of each panel. Horizontal dashed lines signify the summer solstice of each year. White horizontal bands represent periods with no data; from 1998-2007, there were no samples obtained from late fall to early spring because ferries did not operate. Winter GNATS trips were started in 2007. The cruise track is almost east-west, with Portland, ME on the west side and Yarmouth, N.S. on the east side (Fig. 1). Kriged results near ends of the transect should be interpreted with caution due to reduced data coverage and extrapolation of trends (instead of interpolation of trends). Water masses and distance from Yarmouth also shown under X axis. Water masses that are traversed along the transect are also indicated under X axis (see Table 1 for definitions).

Fig. S3-Mean variables measured over Slocum glider missions (10 complete missions; 20 crossings of the GNATS transect). Data binned and averaged over 10m depth increment and 0.1°Longitude. Scale bars for each variable shown to the right of each section. Sections are: (A) Salinity(PSU); (B) Temperature (°C); (C) Density anomaly (sigma-theta); (D) Brunt-Väisälä

Frequency (cycles h^{-1}); (E) DOC (mg C L^{-1}; derived from CDOM fluorescence proxy); (F) POC (mg C L^{-1}; derived from b_{bp532} proxy); (G) mass ratio of DOC:POC; (H) chlorophyll concentration (μg L^{-1}).

Fig. S4- Time series of Gulf-wide absorption measurements of A) CDOM (a_{g412}; m^{-1}) and B) CDOM plus detrital matter (a_{gp412}; m^{-1}) plotted against year. Black diamonds designate the absorption results while open triangles designate the numbers of data points per annual bin. Data only shown for June-September (months where measurements were always made during the GNATS; the time series became year-round in 2006). Data from 2010 are based on a single transect that year due to limited ship availability. Values were anomalously low (marked with a "?"). Vertical error bars around the black diamonds represent standard errors of each cross-Gulf mean.

Fig. S5- Time course of Gulf-wide scattering measurements of A) CDOM (b_{g412}; m^{-1}) and B) CDOM plus detrital matter (b_{gp412}; m^{-1}) plotted against year. Black diamonds designate the absorption results while open triangles designate the numbers of data points per annual bin. Symbols and definitions as in Fig. S4.

Fig. S6- A) Satellite-derived estimates of Gulf-wide DOC concentration (mg C L^{-1}; as determined with MODIS data) plotted against LOADEST estimates of DOC discharge rate from the five largest rivers (Penobscot, Narraguagus, Dennys, St. Croix, and St. John Rivers). (shown in Fig. 1). Satellite-derived DOC concentrations have been lagged by 6 months behind the river discharge rates. B) Correlation (r^2) between Gulf-wide average DOC (determined from satellite-derived a_{g412}) and LOADEST-estimated total DOC discharge (panel A) as a function of lag time (in months).

Fig. S7- Time series of DOC discharge (open squares; based on LOADEST model) from the five largest rivers (as in Fig. S6) and mean satellite-derived, Gulf-wide average DOC concentration (black diamonds; determined from MODIS Aqua satellite using a_{g412} inversion algorithm, extrapolated to [DOC] using regional GNATS relationship). Heavy black lines are six-point (six-month) moving average for each time series (showing the highest correlation; see Fig. S6). Grey error bars around average DOC concentration represent standard error bars within each six-month average.

Fig. S8- Predictions of future annual DOC export from the Penobscot River based on the LOADEST model combined with climate projections for the northeastern US from the United Kingdom Meteorological Office Hadley Centre (HadCM3) [*Gordon et al.*, 2000; *Pope et al.*, 2000] forced with the A1FI emission scenario [*Nakićenović*, 2000]. Model calculations also assume stationarity in the concentration discharge relationship through time. The least squares linear fit suggests a substantial increase in DOC export in the next century.

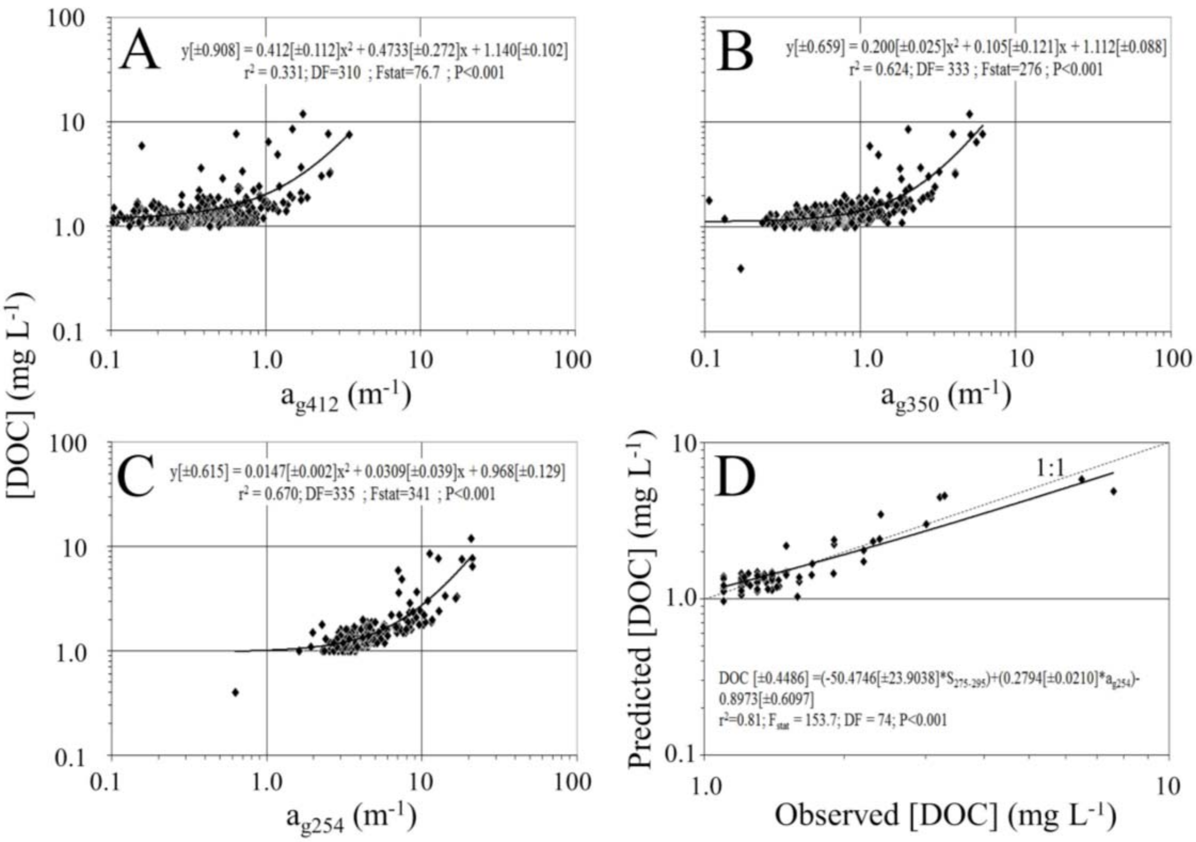

Fig. S1- DOC concentration versus CDOM absorbance measured across the GOM, measured at A) 412nm (a_{g412}), B) 350nm(a_{g350}) and C) 254nm (a_{g254}). D) Predicted DOC using a_{g254} and spectral slope ($S_{275-295}$) plotted against measured DOC concentration for samples collected from the GoM. Grey-shaded region shows data range. Least-squares fits to the data are shown in each panel.

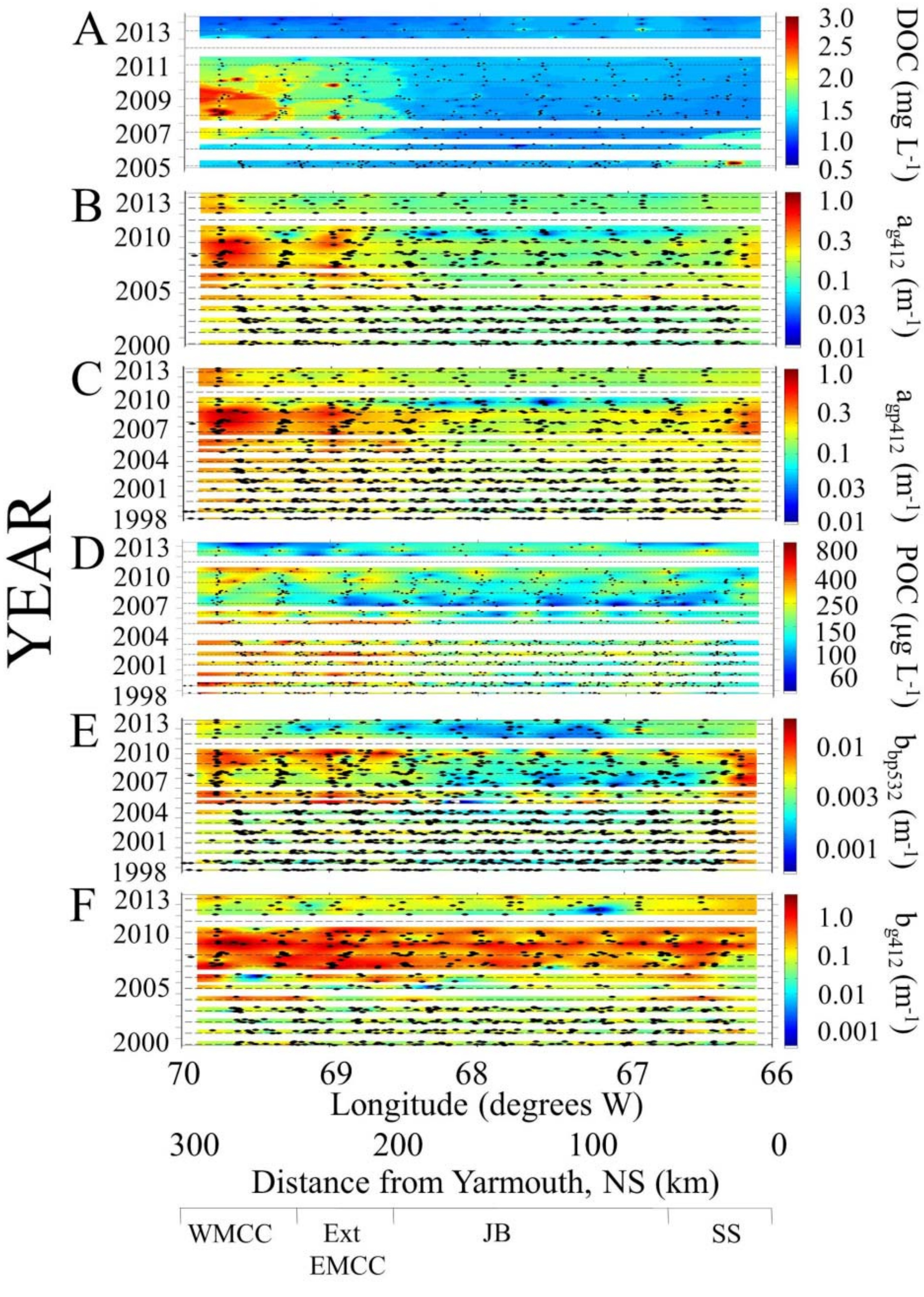

Fig. S2- Hövmoller plots (longitude of east-west GNATS transect versus year) for (A) DOC concentration (mg C L^{-1}), (B) (a_{g412}; m^{-1}), (C) (a_{gp412}; m^{-1}), (D) POC (µg L^{-1}), (E) particulate backscattering at 532nm (b_{bp532}; m^{-1}) and (F) dissolved total scattering at 412nm. Color scale bars shown to right of each panel. Horizontal dashed lines signify the summer solstice of each year. White horizontal bands represent periods with no data; from 1998-2007, there were no samples obtained from late fall to early spring because ferries did not operate. Winter GNATS trips were started in 2007. The cruise track is almost east-west, with Portland, ME on the west side and Yarmouth, N.S. on the east side (Fig. 1). Kriged results near ends of the transect should be interpreted with caution due to reduced data coverage and extrapolation of trends (instead of interpolation of trends). Water masses and distance from Yarmouth also shown under X axis. Water masses that are traversed along the transect are also indicated under X axis (see Table 1 for definitions).

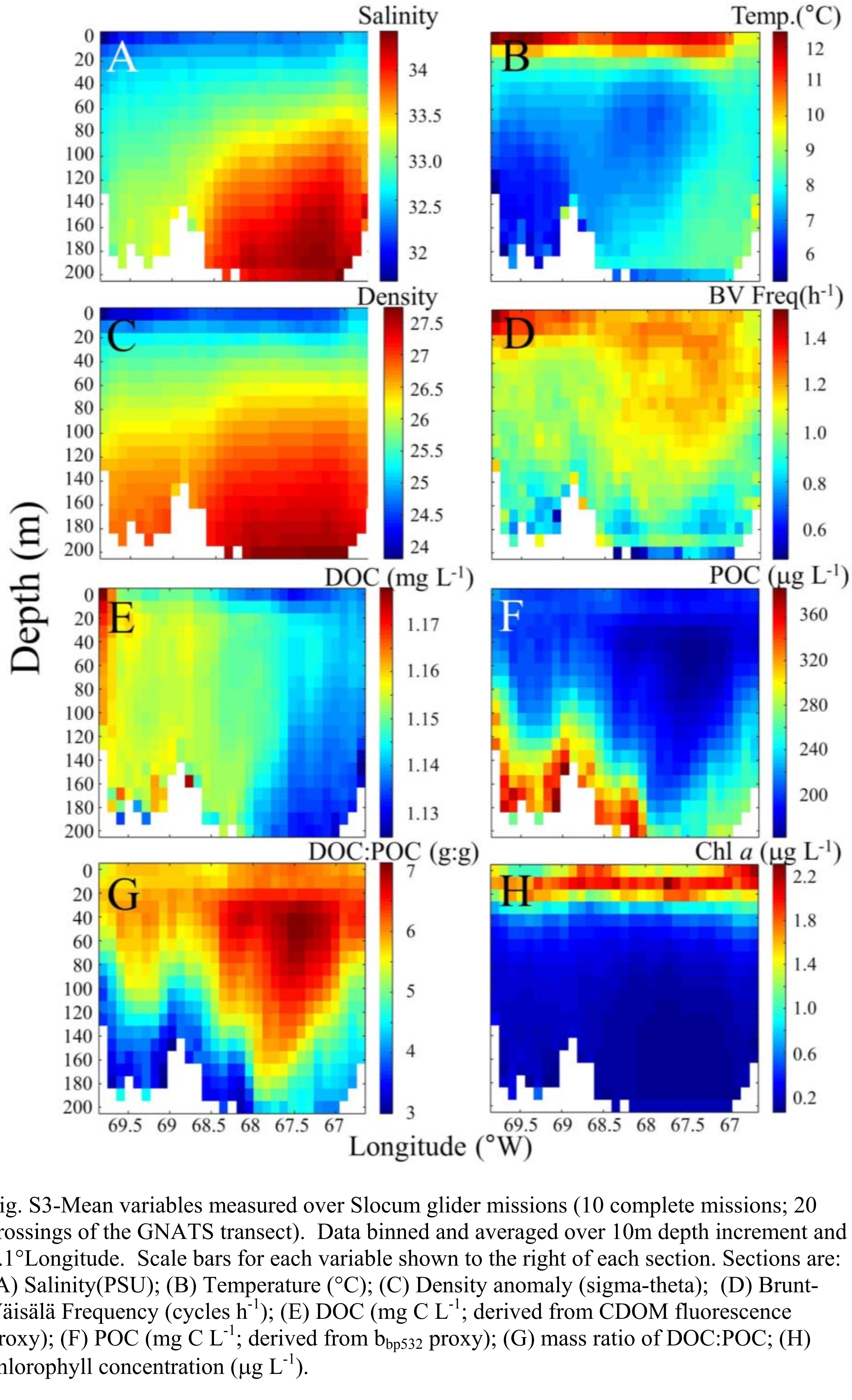

Fig. S3-Mean variables measured over Slocum glider missions (10 complete missions; 20 crossings of the GNATS transect). Data binned and averaged over 10m depth increment and 0.1°Longitude. Scale bars for each variable shown to the right of each section. Sections are: (A) Salinity(PSU); (B) Temperature (°C); (C) Density anomaly (sigma-theta); (D) Brunt-Väisälä Frequency (cycles h^{-1}); (E) DOC (mg C L^{-1}; derived from CDOM fluorescence proxy); (F) POC (mg C L^{-1}; derived from b_{bp532} proxy); (G) mass ratio of DOC:POC; (H) chlorophyll concentration (μg L^{-1}).

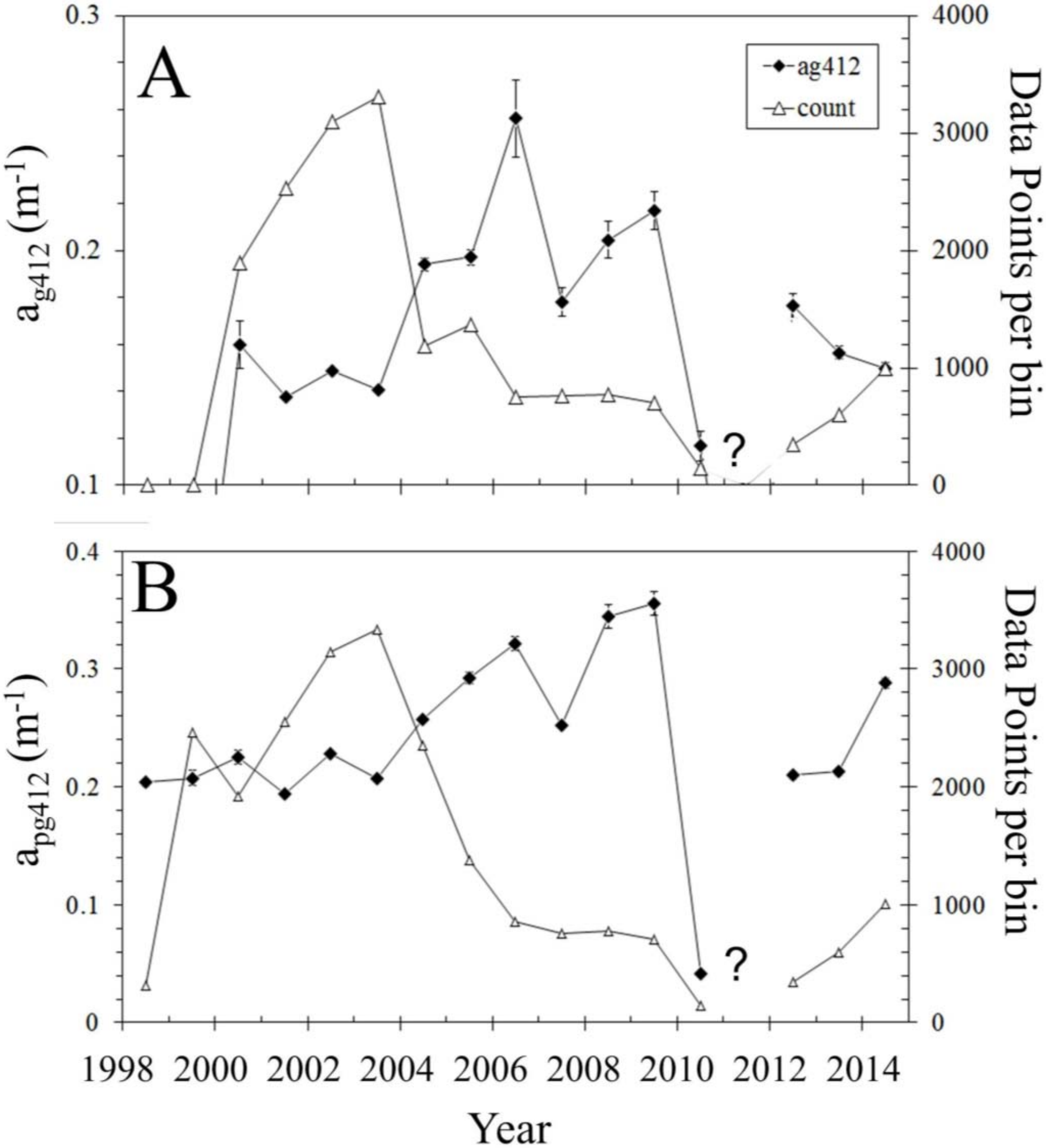

Fig. S4- Time series of Gulf-wide absorption measurements of A) CDOM (a_{g412}; m^{-1}) and B) CDOM plus detrital matter (a_{gp412}; m^{-1}) plotted against year. Black diamonds designate the absorption results while open triangles designate the numbers of data points per annual bin. Data only shown for June-September (months where measurements were always made during the GNATS; the time series became year-round in 2006). Data from 2010 are based on a single transect that year due to limited ship availability. Values were anomalously low (marked with a "?"). Vertical error bars around the black diamonds represent standard errors of each cross-Gulf mean.

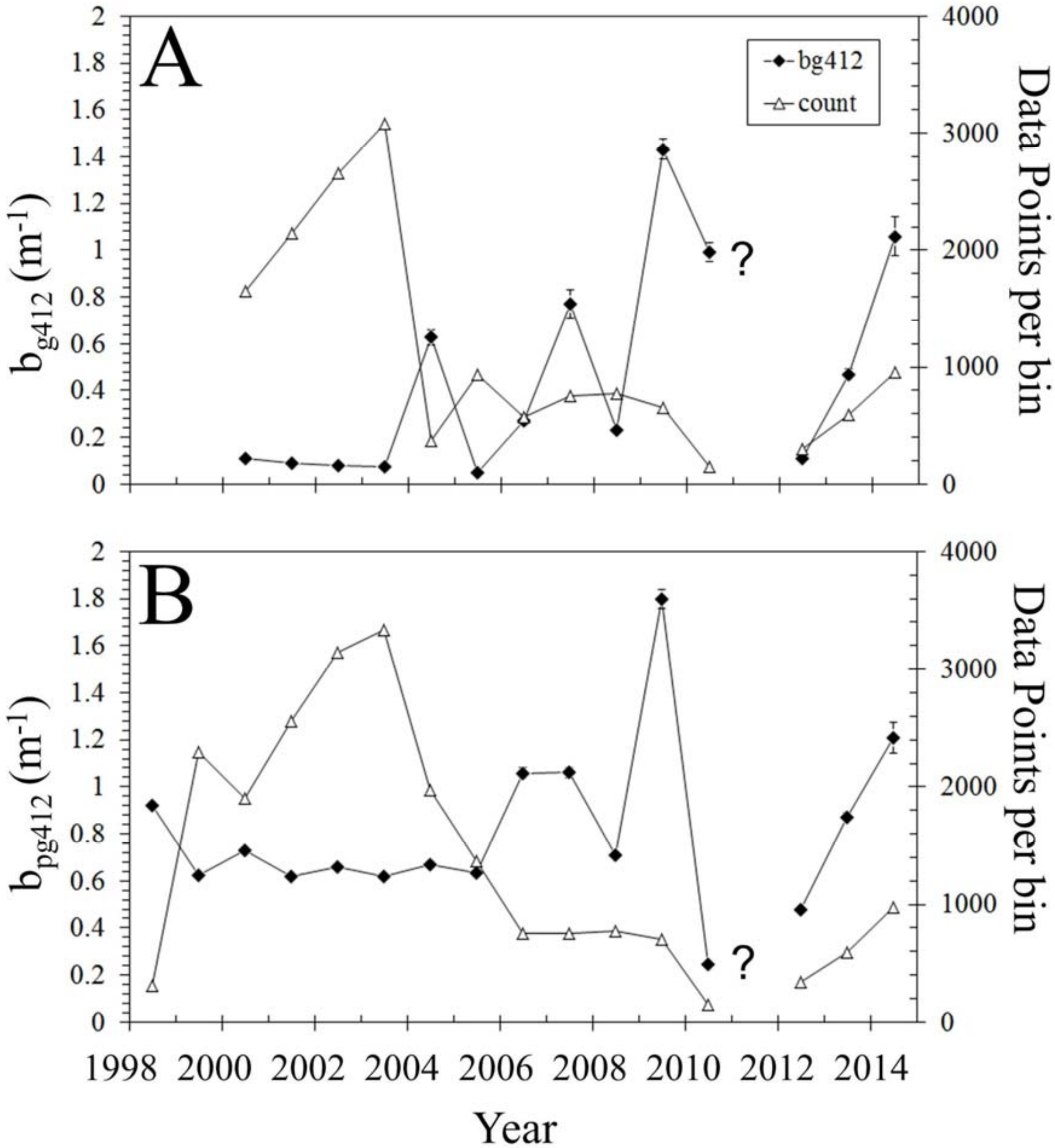

Fig. S5- Time course of Gulf-wide scattering measurements of A) CDOM (b_{g412}; m^{-1}) and B) CDOM plus detrital matter (b_{gp412}; m^{-1}) plotted against year. Black diamonds designate the absorption results while open triangles designate the numbers of data points per annual bin. Symbols and definitions as in Fig. S4.

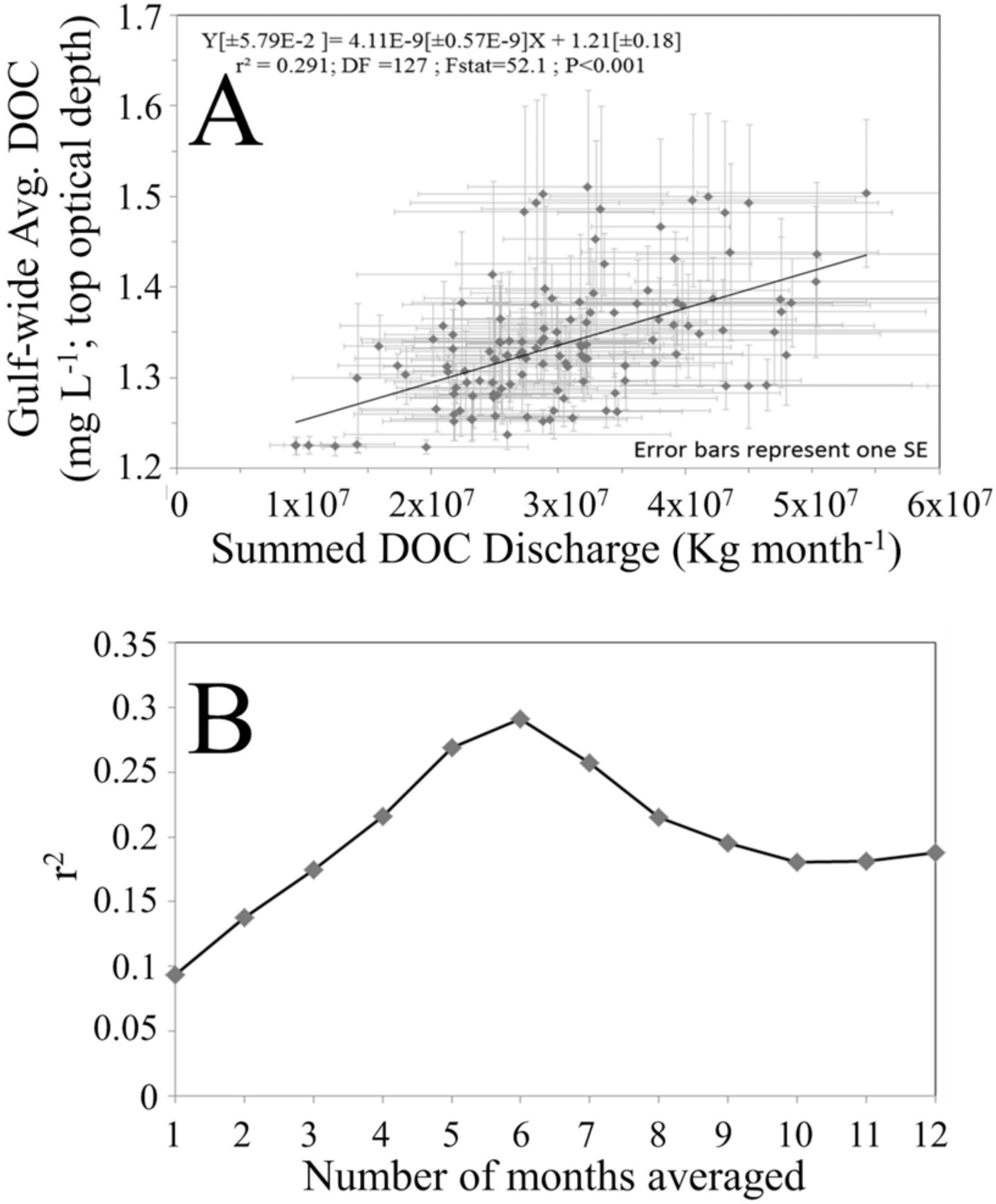

Fig. S6- A) Satellite-derived estimates of Gulf-wide DOC concentration (mg C L^{-1}; as determined with MODIS data) plotted against LOADEST estimates of DOC discharge rate from the five largest rivers (Penobscot, Narraguagus, Dennys, St. Croix, and St. John Rivers as shown in Fig. 1). Satellite-derived DOC concentrations have been lagged by 6 months behind the river discharge rates. B) Correlation (r^2) between Gulf-wide average DOC (determined from satellite-derived a_{g412}) and LOADEST-estimated total DOC discharge (panel A) as a function of lag time (in months).

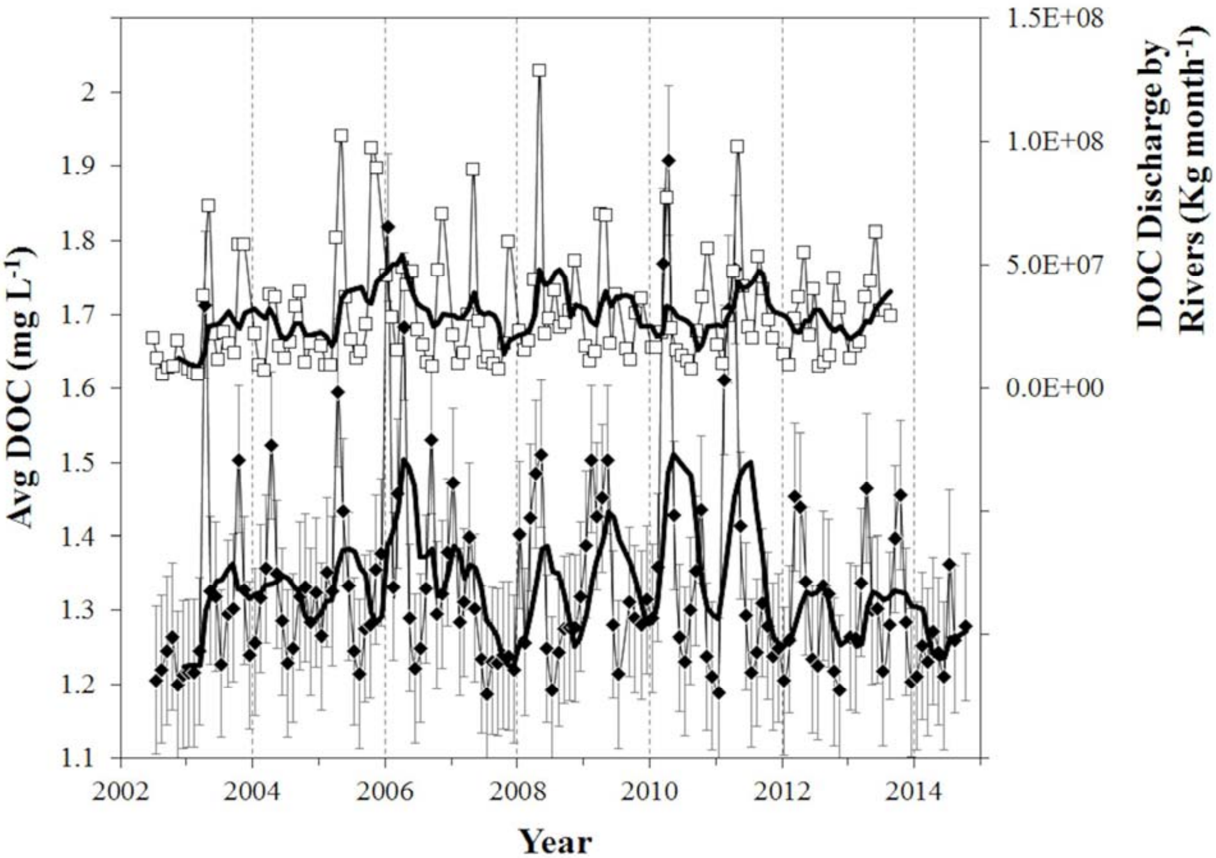

Fig. S7- Time series of DOC discharge (open squares; based on LOADEST model) from the five largest rivers (as in Fig. S6) and mean satellite-derived, Gulf-wide average DOC concentration (black diamonds; determined from MODIS Aqua satellite using a_{g412} inversion algorithm, extrapolated to [DOC] using regional GNATS relationship). Heavy black lines are six-point (six-month) moving average for each time series (showing the highest correlation; see Fig. S6). Grey error bars around average DOC concentration represent standard error bars within each six-month average.

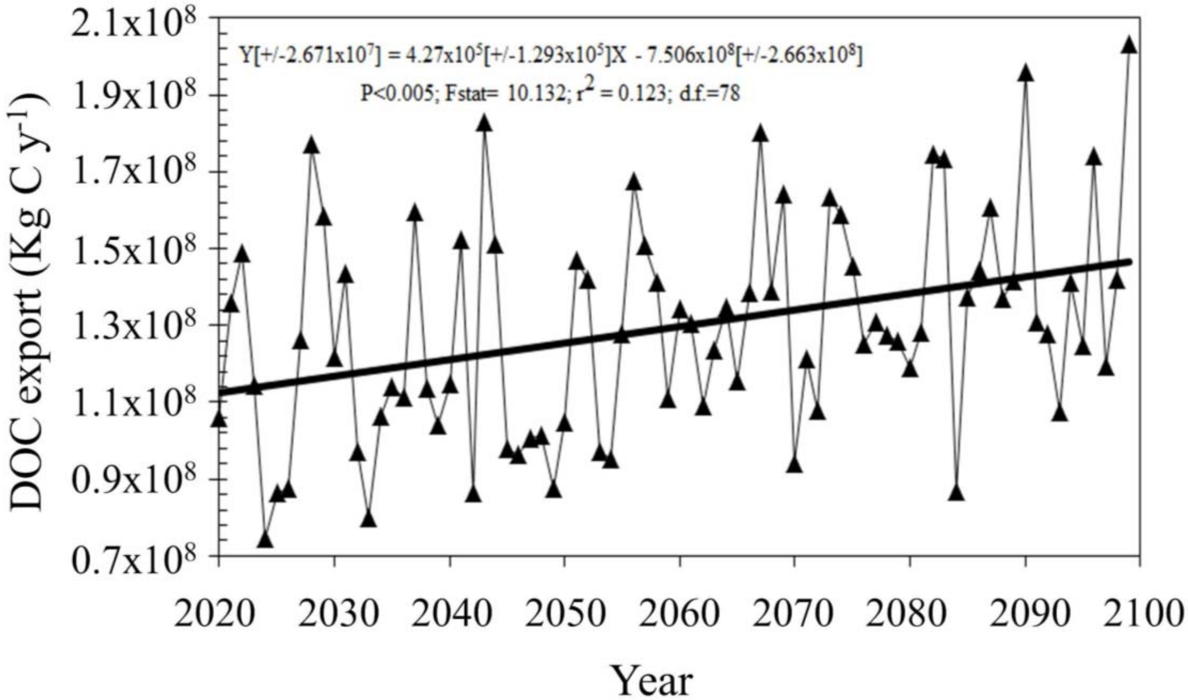

Fig. S8- Predictions of future annual DOC export from the Penobscot River based on the LOADEST model combined with climate projections for the northeastern US from the United Kingdom Meteorological Office Hadley Centre (HadCM3) [*Gordon et al.*, 2000; *Pope et al.*, 2000] forced with the A1FI emission scenario [*Nakićenović*, 2000]. Model calculations also assume stationarity in the concentration discharge relationship through time. The least squares linear fit suggests a substantial increase in DOC export in the next century.